J Mater Sci (2011) 46:3777–3784
DOI 10.1007/s10853-011-5291-4

Study on cell nucleation behavior of HDPE–wood composites/supercritical CO_2 solution based on rheological properties

**Jingjing Zhang · Ghaus M. Rizvi · Chul B. Park ·
Mohammad M. Hasan**

Received: 10 November 2010 / Accepted: 14 January 2011 / Published online: 4 February 2011

Abstract In this study, the shear viscosities of wood–plastic composites (WPC)/supercritical CO_2 (sc-CO_2) solutions at different die temperatures and sc-CO_2 contents were measured by a slit die attached on a single-screw extrusion system. A theoretical model based on the Carreau-Yasuda model and Arrhenius equation was then developed to describe the shear-thinning behavior of the WPC/sc-CO_2 solution. This model was incorporated into a finite element method software, POLYFLOW, to simulate the pressure and velocity field of WPC/sc-CO_2 solution flowing through a foaming die. Based on the simulation results, the pressure drop rate and the location of the supersaturation point were estimated to investigate the cell nucleation. The saturation pressure of sc-CO_2 in WPC was determined by a magnetic suspension balance and corrected by the Sanchez Lacombe Equation of State.

Introduction

The use of wood fiber (WF) as a reinforcing filler in wood–plastic composites (WPC) has attracted a significant amount of attention in recent years. The advantages of WPC are that it has higher stiffness, lower cost, and the fibers are degradable [1]. However, there are a number of drawbacks, such as low impact strength, low ductility, and high density [2], which limit its applications. Foaming of WPC helps to eliminate these drawbacks by creating a large number of uniformly distributed very small cells or bubbles [3].

The WPC foams can be produced by chemical blowing agents (CBA) [4–7], physical blowing agents (PBA) [8–11], or by stretching [12]. The main advantage of CBAs is that these can be used either under high pressure or at atmospheric pressure. However, they are expensive and in WPCs the high temperature requirement for decomposition can have adverse effects on the WF properties, which limits their wide usage. PBAs have no decomposition temperature requirements, have a reduced cost, and generally produce better cell morphology. However, the traditional PBA, such as CFCs and HCFCs, have proven to be detrimental to the Earth's ozone layer, and are being eliminated under the Montreal Protocol. Supercritical fluids are the most favorable replacement due to their unique properties, such as environmental friendliness, non-flammability, and low cost.

The extrusion foaming process, by injecting a supercritical fluid, involves three essential steps: (a) polymer/gas solution formation, (b) cell nucleation, and (c) cell growth. To a large extent, the cell nucleation stage governs the cell morphology of the foams, if the expansion process is controlled properly. Park et al. [13] have showed that a large and rapid die pressure drop is essential for achieving

---

This study was grant sponsored by China Scholarship Council.

J. Zhang (✉)
Faculty of Materials and Energy, Guangdong University of Technology, Guangzhou 510006, People's Republic of China
e-mail: zhangjj@gdut.edu.cn

G. M. Rizvi
Faculty of Engineering and Applied Sciences, University of Ontario Institute of Technology, Oshawa, ON L1H 7K4, Canada

C. B. Park
School of Mechanical and Automotive Engineering, South China University of Technology, Guangzhou 510640, People's Republic of China

C. B. Park · M. M. Hasan
Microcellular Plastics Manufacturing Laboratory, Department of Mechanical and Industrial Engineering, University of Toronto, Toronto, ON M5S 3G8, Canada

a high nucleation rate in the cell nucleation stage, which occurs at the extrusion die. The pressure drop and pressure drop rate are dependent on the shear viscosity of the polymer/gas solution when the die geometry is fixed. Therefore, measuring the shear viscosity of the polymer/gas solution is essential for understanding the foaming process.

To measure the shear viscosity of a polymer/gas solution, the system should be kept under high pressure at all times to prevent phase separation. Therefore, the standard capillary rheometer cannot be used directly. Gerhardt et al. [14] modified a capillary extrusion rheometer for a sealed, high pressure operation to measure the shear viscosity of a PDMS/supercritical CO_2(sc-CO_2) solution. A sc-CO_2 concentration-dependent shift factor was employed to scale both the viscosity and shear rate to a master curve. Later, Gerhardt et al. [15] combined a free volume expression with equation-of-state theories to develop models for the sc-CO_2 concentration-dependent viscoelastic scaling factors. Kwag et al. [16] extended the high-pressure capillary viscometer measurements of Gerhardt et al. [15] to investigate the shear viscosity of polystyrene melts with three soluble gases which are being used for foam manufacturing. The results showed that the viscosity data for all three polystyrene/gas systems follows ideal viscoelastic scaling.

Another methodology can be used to measure the viscosity of a polymer/gas solution: the polymer is melted by the extruder, and then the gas is injected in the extruder and mixed with the polymer to form a polymer/gas solution. Finally, the solution is pumped through the slit or capillary die, while maintaining the pressures above the solubility limit while measuring the pressure changes across the die. Lee et al. [17] applied this methodology to measure the shear viscosity of PS/sc-CO_2 solutions. A linear capillary tube die mounted on a foaming extruder and a back pressure assembly were used. The viscosity data of the PS/sc-CO_2 solution at various pressures, temperatures, and sc-CO_2 contents, were scaled to a master curve. This methodology was also used to measure the shear viscosity of the LDPE/sc-CO_2 solution [18] and the HIPS/nitrogen solution [19] by different authors.

The extrusion foaming of WPC with supercritical fluid has been studied by several researchers. Investigations have been done on the effects of wood content and wood particle size on the cell morphology of foamed WPC by sc-CO_2 [20]. Also the direct relationship between the foaming condition, such as the die temperature and sc-CO_2 content, and final cell morphology were investigated [10, 11]. However, researchers have not studied extensively the fundamental of WPC foaming, such as the shear viscosity of WPC/sc-CO_2 solution and the cell nucleation behavior of WPC.

To better understand the cell nucleation behavior of WPC, this study investigated the pressure drop rate and the location of the supersaturation point during WPC flow through a foaming die at various foaming conditions. The shear viscosity of WPC/sc-CO_2 solutions with 30 wt% WF content was first measured by using a slit die attached to a single-screw extrusion system. Then a viscosity model was developed to describe the shear-thinning behavior of a WPC/sc-CO_2 solution. Finally, this model was incorporated into a finite element method (FEM) software to simulate the pressure and velocity field of WPC flow through a foaming die. Based on the simulation results, the effects of the foaming condition on the cell nucleation stage of foaming WPC were investigated.

Theoretical background

Solubility measurement

A magnetic suspension balance (MSB) was employed to measure the solubility of sc-CO_2 in HDPE melts at 150 °C temperature and pressure up to 28 MPa. The detailed procedure for determining the solubility using the MSB can be found in [21, 22] and is briefly described here. Before beginning the sorption experiment, a precisely weighed polymer sample was placed in the sealed absorption chamber, degassed in the vacuum, and preheated to a designated temperature. The balance readout at vacuum ($P \sim 0$) and temperature (T) for the polymer sample without any dissolved gas was recorded as $W(0, T)$; this value reflected the weight of the sample in vacuum. The high-pressure gas was subsequently charged into the chamber, and sorption occurred. When the saturation stage was reached, the sorption stopped and the weight readout from the balance was recorded as $W(P, T)$ at pressure (P) and temperature (T). Hence, weight gain from the dissolved gas in the polymer, W_g, was calculated as follows:

$$W_g = W(P,T) - W(0,T) + \rho_{gas}(V_B + V_P + V_S), \tag{1}$$

where ρ_{gas} is the gas density; V_B is the volume of the sample holder (including the aluminum sample container and all the metal measuring load coupling devices); V_P is the volume of the pure polymer sample at hydraulic pressure P and temperature T; and V_S is the swollen volume of the polymer/gas mixture caused by the dissolution of gas into the polymer sample. V_B can be determined separately from a blank experiment and V_P can be calculated with the Tait equation of the pure polymer. By ignoring the polymer swollen volume term (V_S) in Eq. 1, the measured weight gain was treated as the apparent weight gain, $W_{g,apparent}$:

$$W_{\mathrm{g,apparent}} = W(P,T) - W(0,T) + \rho_{\mathrm{gas}}(V_{\mathrm{B}} + V_{\mathrm{P}}). \quad (2)$$

The apparent solubility, X_{apparent}, was then derived as:

$$X_{\mathrm{apparent}} = W_{\mathrm{g,apparent}} / \text{ mass of sample}. \quad (3)$$

As shown in Eqs. 1 and 3, it is impossible to measure the accurate solubility of the gas in the polymer melt by ignoring the swollen volume (V_{S}). For the determination of accurate solubility, correction of the buoyancy effect on the apparent solubility data is necessary, especially under a high pressure condition where the gas density (i.e., ρ_{gas}) is high and the swollen volume (i.e., V_{S}) is large. Ideally, the experimental data on the dilation of the polymer during gas sorption will be the most reliable source for determining the swollen volume, V_{S}. However, currently, there is a lack of reliable and accurate PVT data for polymer/gas mixtures which is measured experimentally [23]. Hence, the swollen volume is typically estimated by an equation of state (EOS) which can be applied to a two-component mixture system under equilibrium. In this study, the Sanchez-Lacombe (SL) EOS was used to investigate the fluid phase equilibria, where the theoretical solubility, X_{theory}, and the swollen volume of polymer, V_{S}, were determined quantitatively. The details of the SL EOS can be found in our previous studies [21, 22].

Once the swollen volume (V_{S}) is known, the corrected solubility, $X_{\mathrm{corrected}}$, with the buoyancy effect compensation was obtained as:

$$X_{\mathrm{corrected}} = X_{\mathrm{apparent}} + \left(\rho_{\mathrm{gas}} \mathrm{x}\ V_{\mathrm{S}}\right) / \text{mass of sample}. \quad (4)$$

For WPC, since the WF almost does not absorb any gas, the solubility of gas in WPC can be approximately determined from the solubility of gas in polymer [24].

$$X_{\mathrm{WPC}} = X_{\mathrm{corrected}} \times C_{\mathrm{HDPE}}, \quad (5)$$

where C_{HDPE} is the mass content of polymer in WPC.

Relationship between the free volume and the viscosity

The plasticizing effect of the dissolved gas can be attributed to an increase of the free volume and by a real dilution effect [25]. The contribution of free volume was first proposed by Doolittle [26] by relating viscosity with the free volume fraction. Kelley and Bueche [27] justified the validity of the Doolittle equation in a polymer-diluent system and expressed that there is a concentrated dependence of the viscosity on polymer-diluent system. Young [28] calculated the free volume fraction of the solution based on a simple mixing rule with the contribution of each component weighted by its volume fraction. Areerat et al. [18] calculated the free volume fractions of LDPE/sc-CO_2 solutions by the SL EOS and the solubility data was measured by a MSB.

Experimental

Materials

The polymer was high density polyethylene (HDPE) 2710, supplied by Nova Chemicals. The WF was standard softwood (pine) with grade of 12020, supplied by American WFs. Maleic anhydride-g-HDPE (Fusabond MB-100D, MFI = 2.0 g/10 min) was used as coupling agent, supplied by DuPont Canada. Lubricant (TPW 113) was supplied by Struktol America. The CO_2, with 99.5% purity, was supplied by BOC Gas Co.

Compounding

Before mixing, the WF was oven dried at 100 °C for 12 h to remove moisture from the wood. The mixing ratio of HDPE:WF:coupling agent:lubricant was 70:30:3:3 (phr). All these materials were dry-blended and then were mixed in a co-rotating twin screw extruder (Leistritz Co.) with a screw diameter of 27 mm, and a length-to-diameter ratio of 40. The screw configuration was designed to provide dispersive and distributive mixing for dispersing the WF in the HDPE uniformly [29]. The barrel temperature was set at 150 °C, and the die temperature was set at 160 °C. The screw speed was set at 100 rpm. The extruded strands were cooled in water and then pelletized. These pellets were dried at 100 °C for 12 h and then used for viscosity measurement.

Viscosity measurement

The viscosity of WPC/sc-CO_2 solution was measured by a slit die attached to a single-screw extrusion system, as shown in Fig. 1. The detailed procedure for determining the shear viscosity using the slit die can be found in [30]. A resistance nozzle was attached downstream of the slit die to maintain a high pressure in the slit die [17].

The extrusion system consisted of a 5 hp extruder drive with a speed-control gearbox, a ¾″ single-screw extruder (Brabender 05-25-000), a gas-injection equipment (ISCO pumps 260D), a dissolution-enhancing device containing static mixers (Omega FMX8441S), a heat exchanger containing static mixers (Labcore H-04669-12). The dissolution-enhancing device and heat exchanger are used to promote the homogeneous dissolution of gas into the plastic melt and cooling the melt, respectively.

The temperatures in the single screw extruder were maintained at 80, 150, and 150 °C in zones 1, 2, and 3, respectively. The temperature of the dissolution-enhancing device, heat exchanger, slit die, and nozzle were all set at 150 °C at first. Then sc-CO_2 was injected into the WPC melt, and those temperatures were reduced at an interval of

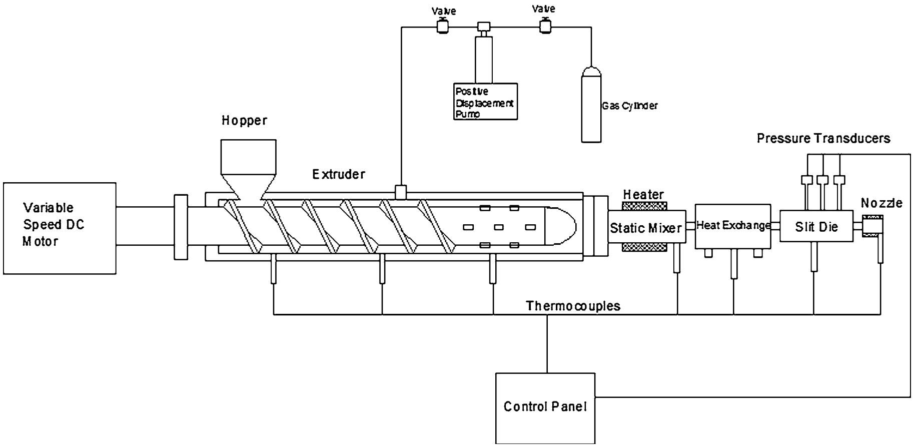

Fig. 1 Schematic of the extruder setup for the measurement of the WPC/sc-CO_2 solution viscosities

5 °C from 150 to 135 °C. The pressure and volume flow rate were recorded at each 5 °C intervals from 150 °C when the stable processing conditions were obtained. At each temperature, the content of sc-CO_2 in WPC used was 1, 2, and 3 wt%.

Experimental results and discussion

Table 1 shows the saturation pressure of HDPE and WPC at different sc-CO_2 contents and the temperature of 150 °C. Higher pressure was required to dissolve more gas for both the HDPE and WPC. Moreover, it can be seen that WPC needs a higher saturation pressure than that for HDPE to dissolve the same amount of sc-CO_2, since WF cannot absorb gas. Therefore, to form WPC/sc-CO_2 solutions in the slit die at all testing conditions, the pressure inside the slit die should be higher than the saturation pressure of this solution at 3% sc-CO_2.

As mentioned earlier, the pressure inside the slit die should be kept high enough to prevent phase separation. The axial pressure drop profiles of the WPC/sc-CO_2 solution along the slit channel need to be checked to satisfy the condition. The results were shown in Fig. 2. It can be clearly seen that the pressure drop profiles were linear for the composites with different sc-CO_2 contents which indicates that phase separation did not occur. Either P1–P2 or P2–P3 can be used as the pressure drops to calculate the shear stress. Also the pressures of the composites with different sc-CO_2 contents were higher than their corresponding saturation pressure. This confirmed that the WPC/sc-CO_2 solution was formed and no phase separation occurred during the measurement.

Table 1 The saturation pressure of HDPE and WPC at different sc-CO_2 contents and the temperature of 150 °C

CO_2 content (%)	Saturation pressure (MPa)	
	HDPE	WPC with 30 wt% WF
1	1.5	2.1
2	3.0	4.3
3	4.5	6.4

The viscosity curves have been determined for WPC/sc-CO_2 solutions at three sc-CO_2 contents (1, 2, and 3%) and three die temperatures (135, 140, and 145 °C) after a Rabinowitsch correction, as shown in Fig. 3, respectively. The plasticization effect of the dissolved sc-CO_2 was obvious for WPC. The more the gas dissolved, the lower the shear viscosity was. Also the shear viscosities of the WPC/sc-CO_2 solution increased with decreased temperature. All the shear viscosity curves of the WPC/sc-CO_2 solutions showed typical shear-thinning behaviors. Thus, the shear viscosity of the WPC/sc-CO_2 solutions can be described by the Carreau-Yasuda model.

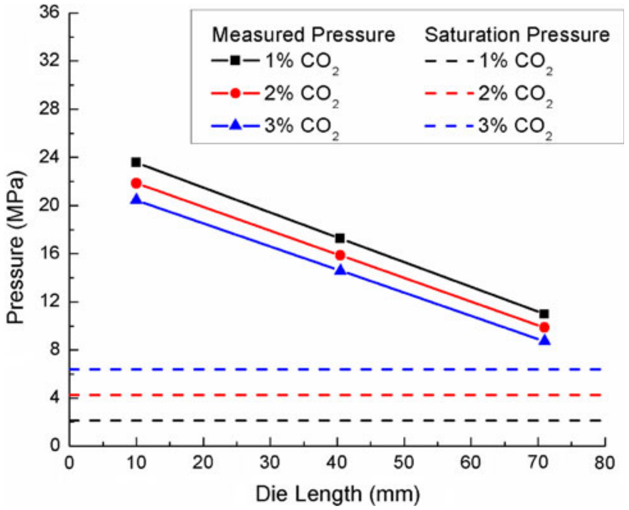

Fig. 2 The axial pressure drop profiles of the WPC/sc-CO2 solution along the slit channel

Fig. 3 The shear viscosity of the WPC/sc-CO_2 solution at different die temperatures: **a** 145 °C, **b** 140 °C, and **c** 135 °C

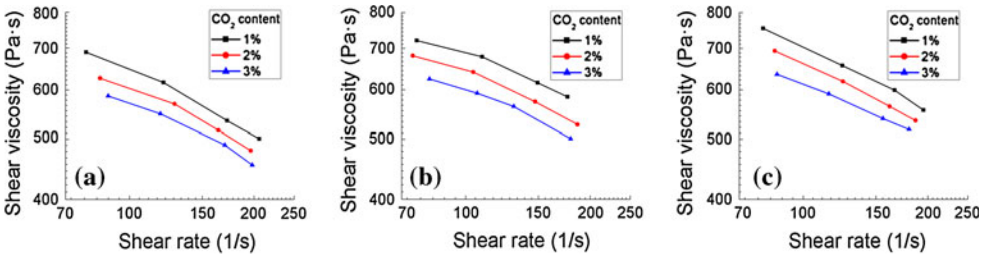

$$\eta = \eta_\infty + \frac{\eta_0 - \eta_\infty}{[1 + (\lambda\dot{\gamma})^a]^{\frac{(1-n)}{a}}}, \tag{6}$$

where η, η_∞, and η_0 are the shear, infinite-shear, and zero-shear viscosity, respectively. $\dot{\gamma}$ is the shear rate. n, a, and λ are parameters, which govern the behavior of the power law region of the viscous behavior.

For the WPC/sc-CO_2 solution, $\eta_\infty \ll (\eta, \eta_0)$ can hold and Eq. 6 can be simplified into

$$\eta = \frac{\eta_0}{[1 + (\lambda\dot{\gamma})^a]^{\frac{(1-n)}{a}}}. \tag{7}$$

From Fig. 3, it can be noted that the slope of the viscosity curve was not greatly changed at different sc-CO_2 contents and temperatures. It is expected that the effect of temperature, pressure, and sc-CO_2 content on the shear viscosity of a polymer/gas solution can be reflected through the zero-shear viscosity. Therefore, based on the free volume theory, the zero-shear viscosity can be expressed in an Arrhenius form.

$$\eta_0 = A'\exp\left(\frac{B'}{f}\right) = A\exp\left(\frac{\alpha}{T - T_r} + \beta P + \psi C\right), \tag{8}$$

where T, P, and C are temperature, pressure and gas content, respectively. T_r is reference value of temperature. f is the fractional free volume, and A', B', A, α, β, and ψ are characteristic parameters determined by the polymer/gas solution. Thus, the shear-thinning behavior of the WPC/sc-CO_2 solution can be described by combining Eqs. 7 and 8.

When the shear viscosity data were fitted into both the Carreau-Yasuda model (Eq. 7) and Arrhenius equation (Eq. 8), the values of the characteristic parameters of the viscosity model were determined, as shown in Table 2. By using these parameters, the shear viscosity data can be downward shifted to a master curve of η/η_0 versus $\eta_0\dot{\gamma}$, as plotted in Fig. 4. It can be seen that the shifted viscosity data of the WPC/sc-CO_2 solution fit the theoretical model quite well. This indicated that the shear thinning behavior of the WPC/sc-CO_2 solution can be described adequately by the Carreau-Yasuda model and Arrhenius equations. From Table 2, it is noted that the power law index n was far below one, which indicated the significant non-Newtonian behavior of the WPC/sc-CO_2 solution. The concentration coefficient, ψ, was negative and demonstrated the plasticization effect of sc-CO_2.

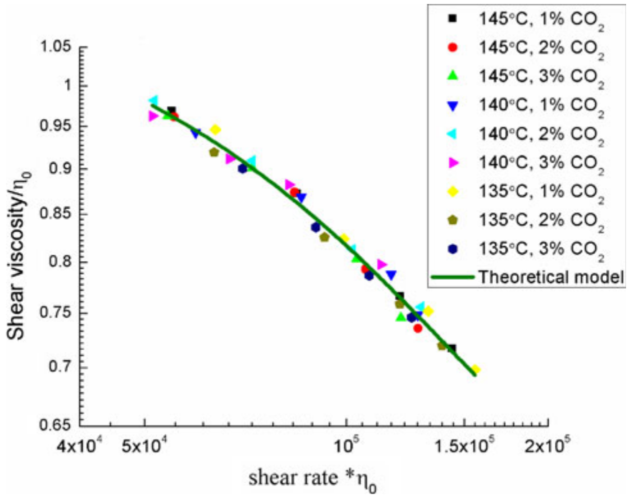

Fig. 4 Master curve of the shear viscosity of WPC/sc-CO_2 solution

Table 2 Fitting parameters of the WPC/sc-CO_2 solution viscosity model

T_r (K)	n	a	λ	ψ	β (Mpa^{-1})	α (K)	A
308.47	0.5455	3.5600	0.0101	−6.6539	0.0015	142.74	199.99

Simulation condition

To investigate the cell nucleation behavior of WPC/sc-CO_2 solutions that flow through a foaming die, a FEM software, POLYFLOW (a software package from FLUENT Inc.), was used to simulate the flow field in the die. The flow channel of the foaming die consisted of a die insert section, a converging section and a capillary section. The die insert section has a length of 5 mm and an internal diameter of 10 mm, and the capillary section has a length of 20 mm and an internal diameter of 1 mm. The converging angle between the die insert section and the capillary section is 120°, which helps to suppress recirculation. The geometry model and the mesh of the foaming die were created by GAMBIT (a software package from FLUENT Inc.), as shown in Fig. 5a and b, respectively. The mesh of the

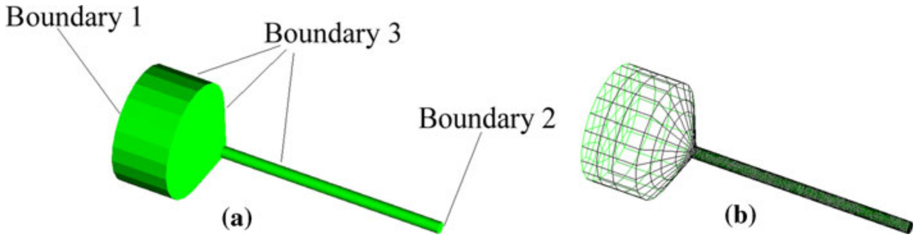

Fig. 5 **a** Geometry model and **b** mesh of the simulated foaming die

model is very important, because it determines the precision of the simulation results and the simulation time. Fine mesh results in higher precision results but longer simulation time. In this model, the capillary section dominates the flow characteristic, and the die insert section does not significantly affect the flow in the capillary section. So, the finer mesh was created in the capillary section, while the wide mesh was created in the die insert section. The final mesh contains 9176 hexagon element.

Since POLYFLOW cannot handle two-phase flows, it is assumed in the simulation that the phase separation in the die does not significantly affect the flow field in the die. In order to simplify the simulation, another assumption was also made: (1) the flow of the WPC/sc-CO_2 solution in the die was treated as steady, fully developed and with a generalized Newtonian isothermal flow. No wall slip was detected; (2) the WPC/sc-CO_2 solution was incompressible; (3) the effects of gravity and inertial force were ignored.

The aforementioned viscosity model based on both the Cross-Yasuda model (Eq. 7) and Arrhenius equation (Eq. 8) was incorporated in the POLYFLOW software to characterize the shear-thinning behavior of the WPC/sc-CO_2 solution. The constant parameter of the viscosity model was obtained by fitting the experimental data to the viscosity model, as shown in Table 2. The conservation equations used in the simulation were expressed in tensor notation:

Continuity Equation:

$$\frac{\mathrm{D}\rho}{\mathrm{D}t} + \rho(\nabla \cdot \upsilon) = 0, \tag{9}$$

where ρ is density, υ is velocity. Since the WPC/sc-CO_2 solution was assumed to be incompressible, the density is constant, thus $\frac{\mathrm{D}\rho}{\mathrm{D}t} = 0$.Momentum Equation:

$$\rho a = -\nabla P + \nabla \cdot T + f, \tag{10}$$

where a is acceleration, P is pressure, T is extra-stress tensor, and f is volumetric force. No energy equation is needed to be solved because an isothermal flow is assumed.

The boundary of the model is also shown in Fig. 5a. The flow boundary condition is defined as follows: The boundary 1 is an inflow where volumetric flow rate is set at 3.35×10^{-8} m^3/s. The boundary 2 is an outflow, which is defined as a zero normal force and a zero tangential force. The boundary 3 is a flow channel, which is defined as a zero normal velocity and a zero tangential velocity due to the absence of the wall slip.

Post processing was performed with FLPOST (a software package from FLUENT Inc.). The pressure and velocity field were obtained. In addition, particle tracking methods were used to obtain the path line.

Simulation results and discussion

The effect of the die temperature on the flow behavior for the WPC in 1 wt% sc-CO_2 concentration was investigated. The pressure and velocity values on the centerline were used to quantitatively characterize this effect. The results are shown in Fig. 6. From Fig. 6a, it can be seen that by decreasing the die temperature, both the pressure and pressure drop increased due to the high viscosity of the WPC in low temperatures. The saturation pressure of 1 wt% sc-CO_2 in the WPC, the horizontal dashed line, is also shown in Fig. 6a to determine the location of the supersaturation point. In the region above this dashed line, the WPC can maintain 1 wt% sc-CO_2. On the contrary,

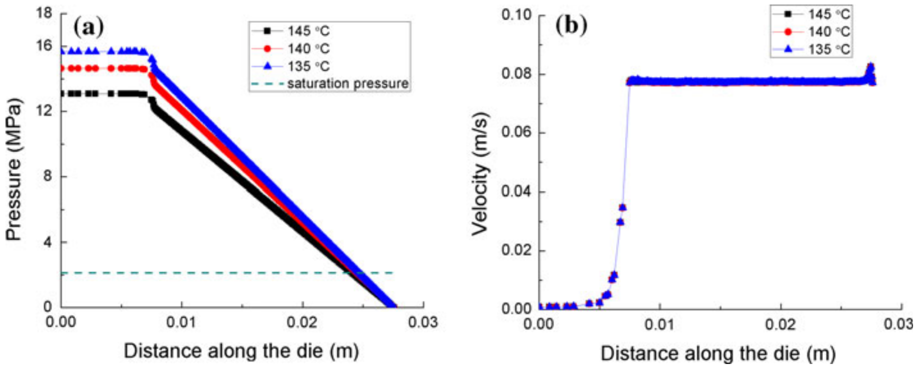

Fig. 6 The simulated **a** pressure profile and **b** velocity profile of the WPC/sc-CO_2 solution flow through the foaming die at different die temperatures. The sc-CO_2 concentration is 1%

below this dashed line, the WPC will be supersaturated with 1 wt% sc-CO_2. Thus, the intersection of the pressure profile and the dashed line represents the onset position where the solution becomes saturated. This position can be theoretically considered as the point where bubble nucleation can begin. For the three die temperatures, when the die temperature decreases, the position of supersaturation point shifts toward the die exit, which means that the cell growth time inside the die is the shortest for WPC's at 135 °C. Since the high shear rate inside the die will stretch the bubble, a short cell growth time is a benefit to the cell structure. Therefore, decreasing the die temperature is of benefit to cell nucleation, because it increases the die pressure and moves the supersaturation point closer to the die exit.

From Fig. 6b, it can be seen that the velocity profiles are the same at three die temperatures. It should be noticed that the volumetric flow rate of the inflow was set at the same value in the simulation, which caused the same velocity as long as the die geometry was fixed. In reality, the volumetric flow rate may have some difference at different die temperatures due to the leakage flow in the barrel caused by high pressures at low die temperatures.

The residence time distribution was then calculated in the domain where a velocity field had been calculated. The residence time was set to zero on the inflow boundary. After the residence time was calculated, pressure drop rate could be obtained. The simulated residence time and pressure drop rate of the WPC/sc-CO_2 solutions at different die temperatures are shown in Table 3. It can be seen that the pressure drop rate increases by decreasing the die temperature. This demonstrated that decreasing the die temperature is of benefit to cell nucleation.

The effect of the sc-CO_2 content on the pressure along the centerline was then investigated, as shown in Fig. 7. The velocity profile is not included, because the sc-CO_2 content will not influence the velocity profile when the inflow volumetric flow rate is the same. The pressure drop rates of the WPC/sc-CO_2 solution for different sc-CO_2 contents are also shown in Table 3. The simulated pressure drop and pressure drop rate decreased with the increase of the sc-CO_2 content due to the plasticization effect of sc-CO_2. To dissolve more sc-CO_2, higher saturation pressure was needed. Comparing to the intersection of each pressure profile and its corresponding saturation pressure line, it can be seen that the position of the supersaturation point moves inwards and away from the die exit when the sc-CO_2 content was increased.

Table 3 The simulated residence time and pressure drop rate of the WPC/sc-CO_2 solution at different die temperatures and sc-CO_2 contents

	Residence time in the capillary section(s)	Pressure drop rate (MPa/s)
WPC at 145 °C and 1% CO_2	0.55	23.78
WPC at 140 °C and 1% CO_2	0.55	26.61
WPC at 135 °C and 1% CO_2	0.55	28.49
WPC at 135 °C and 2% CO_2	0.55	25.32
WPC at 135 °C and 3% CO_2	0.55	23.64

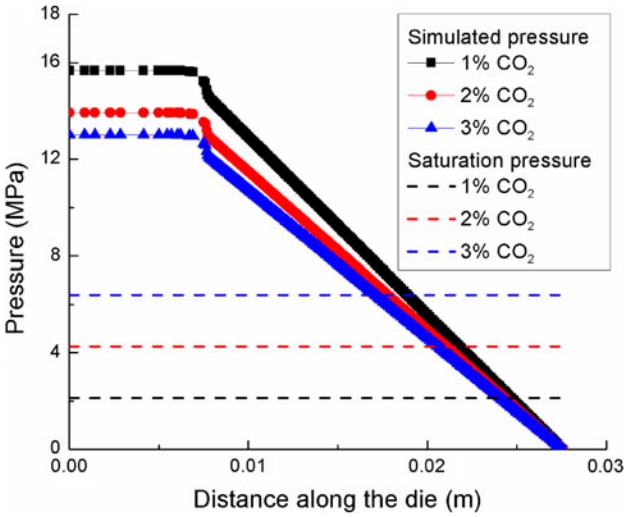

Fig. 7 The simulated pressure profile of the WPC/sc-CO_2 solution flow through the foaming die at different sc-CO_2 contents. The die temperature is 145 °C

A higher sc-CO_2 content creates large supersaturation ratios for nucleation, which can nucleate more bubbles. However, a higher sc-CO_2 content causes lower pressure drop and pressure drop rates, which induces a less thermodynamic instability. Also a higher sc-CO_2 content causes earlier onset of the nucleation inside the die away from the exit, which causes a longer cell growth time inside the die. Therefore, too high sc-CO_2 content will not be desirable to obtain a good cell structure.

Conclusions

In this study, an experimental study of the shear viscosities of WPC/sc-CO_2 solutions at three sc-CO_2 contents (1, 2, and 3%) and three die temperatures (135, 140, and 145 °C) was performed. The significant plasticization effect of the dissolved sc-CO_2 could be observed. The effects of temperature, pressure, and sc-CO_2 content were modeled using the Carreau-Yasuda model and Arrhenius Equation. Then a simulation was conducted for the flow of the WPC/sc-CO_2 solution through a foaming die using the proposed viscosity model. The pressure field and velocity field were determined from the simulation. The saturation pressure of the sc-CO_2 in WPC was determined by an MSB and corrected by SL EOS. Based on this information, the pressure drop rate and the position of the supersaturation point were used to investigate the effect of die temperature and sc-CO_2 content on cell nucleation. The results showed that lower die temperatures induced high pressure drop rates and shifted the position of the supersaturation point toward the die exit, which, therefore, should promote small and regular cell structures. By increasing the sc-CO_2 content, a large supersaturation ratio was created, but higher sc-CO_2 content also caused the position of supersaturation point to be farther away from the die exit, and this can degrade cell morphology.

References

1. Klyosov AA (2007) Wood-plastic composites. Wiley, Hoboken
2. Bledzki AK, Faruk O, Huque M (2002) Polym-Plast Technol 41:435
3. Martini J, Waldman F, Suh NP (1982) SPE ANTEC, San Francisco: 674
4. Bledzki AK, Faruk O (2006) Cell Polym 25:143
5. Bledzki AK, Faruk O (2006) J Cell Plast 42:63
6. Bledzki AK, Faruk O (2006) J Cell Plast 42:77
7. Li Q, Matuana LM (2003) J Appl Polym Sci 88:3139
8. Matuana LM, Park CB, Balatinecz JJ (1997) Polym Eng Sci 37:1137
9. Rizvi GM, Park CB, Lin WS, Guo G, Pop-Iliev R (2003) Polym Eng Sci 43:1347
10. Zhang H, Rizvi GM, Park CB (2004) Adv Polym Technol 23:263
11. Guo G, Lee YH, Rizvi GM, Park CB (2005) SPE ANTEC, Boston: 92
12. Kim YS, Guo G, Wang KH, Park CB, Maine FW (2004) SPE ANTEC, Chicago: 1608
13. Park CB, Baldwin DF, Suh NP (1995) Polym Eng Sci 35:432
14. Gerhardt LJ, Manke CW, Gulari E (1997) J Polym Sci Polym Phys 35:523
15. Gerhardt LJ, Garg A, Manke CW, Gulari E (1998) J Polym Sci Polym Phys 36:1911
16. Kwag C, Manke CW, Gulari E (1999) J Polym Sci Polym Phys 37:2771
17. Lee M, Park CB, Tzoganakis C (1999) Polym Eng Sci 39:99
18. Areerat S, Nagata T, Ohshima M (2002) Polym Eng Sci 42:2234
19. Chong TH, Ha YW, Jeong DJ (2003) Polym Eng Sci 43:1337
20. Guo G, Lee YH, Rizvi GM, Park CB (2008) J Appl Polym Sci 107:3505
21. Li G, Li H, Wang J, Park CB (2006) Cell Polym 25:237
22. Li G, Wang J, Park CB, Simha R (2007) J Polym Sci Polym Phys 45:2497
23. Li YG, Park CB, Li HB, Wang J (2008) Fluid Phase Equilib 270:15
24. Cheremisinoff NP (1989) Handbook of polymer science and technology. Marcel Dekker, New York
25. Ferry JD (1970) Viscoelastic properties of polymers. Wiley, New York
26. Doolittle AK (1951) J Appl Phys 22:1471
27. Kelley FN, Bueche F (1961) J Polym Sci 50:549
28. Bae YC (1996) Polymer 37:3011
29. Zhang J, Park CB, Rizvi GM, Huang H, Guo Q (2009) J Appl Polym Sci 113:2081
30. Wang J, Park CB, James DF (2007) SPE ANTEC, Cincinnati: 1948